

Vision Learners Meet Web Image-Text Pairs

Bingchen Zhao^{1,3} Quan Cui^{2,3} Hao Wu^{3†} Osamu Yoshie² Cheng Yang³
¹University of Edinburgh ²Waseda University ³Bytedance

zhaobc.gm@gmail.com cui-quan@toki.waseda.jp wuhao.5688@bytedance.com

Abstract

Most recent self-supervised learning (SSL) methods are pre-trained on the well-curated ImageNet-1K dataset. In this work, we consider SSL pre-training on noisy web image-text paired data due to the excellent scalability of web data. First, we conduct a benchmark study of representative SSL pre-training methods on large-scale web data in a fair condition. Methods include single-modal ones such as MAE and multi-modal ones such as CLIP. We observe that multi-modal methods cannot outperform single-modal ones on vision transfer learning tasks. We derive an information-theoretical view to explain the benchmarking results, which provides insights into designing novel vision learners. Inspired by the above explorations, we present a visual representation pre-training method, MULTI-modal Generator (MUG), for scalable web image-text data. MUG achieves state-of-the-art transferring performances on a variety of tasks and shows promising scaling behavior. Models and codes will be made public.¹

1. Introduction

Self-supervised representation learning (SSL) approaches have attracted considerable attention recently because SSL could reduce the reliance on labor-intensive human annotation. The design of SSL methods is mainly guided by the InfoMax principle [23], which shows that maximizing the mutual information $I(X; T)$ of the input data X and the learned representation T can lead to better representations. Contrastive learning [4, 7–10, 18, 36] and masked image modeling [2, 3, 17, 31, 46] within the image modality can learn transferrable representations from data by solving pre-defined pretext objectives that aim to optimize $I(X; T)$, achieving state-of-the-art results on popular computer vision benchmarks. Despite remarkable advancements, most SSL methods are developed on the ImageNet-1K [13] dataset, which is well-curated.

[†]Corresponding author.

¹Demo available at https://huggingface.co/spaces/tennant/MUG_caption

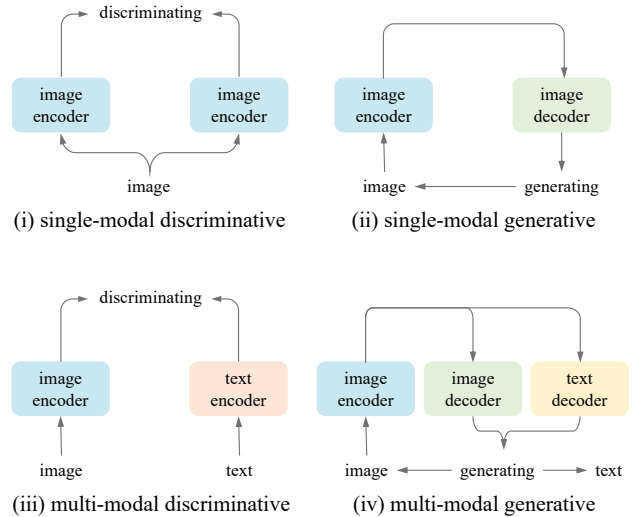


Figure 1. Comparison of vision encoder pre-training paradigms with image-text pairs. Four paradigms are considered, *i.e.*, (i) single-modal discriminative (*e.g.*, SimCLR [7]), (ii) single-modal generative (*e.g.*, MAE [17]), (iii) multi-modal discriminative (*e.g.*, CLIP [32]), and (iv) multi-modal generative (**our proposed MUG**). Multi-modal generative paradigm simultaneously generates images and texts with only image representations.

This fashion cannot reflect the scalability of the SSL methods, *e.g.*, several methods are only evaluated on the ImageNet-1K dataset [17, 18, 51].

Differing from the above single-modal SSL methods, pioneering multi-modal SSL methods (CLIP [32] and ALIGN [24]) have shown great scalability, *i.e.*, easily collected large-scale web image-text pairs [34, 35, 38] can contribute to great transfer learning performances. The following works also proved that the textual information in web image-text pairs could greatly benefit various downstream tasks [26, 27, 30, 54]. *In a fair condition*, with the same web image-text dataset and training schedule, we first conduct a benchmark study of single-modal SSL methods (with only images) and multi-modal SSL methods (with image-text pairs). However, we observe that the representation learned from multi-modal SSL methods cannot outperform single-modal SSL ones on the most representative computer

vision task: ImageNet-1K end-to-end fine-tuning.

Driven by the benchmark study, we investigate how to design a multi-modal SSL paradigm, which can achieve superior transferring performances to single-modal SSL methods with web image-text pairs. In Fig. 1 (i-iii), we categorize previous representative methods as three types, single-modal discriminative (e.g., SimCLR [7]), single-modal generative (e.g., MAE [17]), and multi-modal discriminative (e.g., CLIP [32]). Based on our benchmark study, we have two key observations. First, generative methods achieve the best transfer performances. Second, multi-modal methods cannot outperform single-modal methods. To explain the observations, we further present an information-theoretical derivation. The derivation takes the InfoMax principle [23] for learning representations, and the information-bottleneck theory is introduced to explain the transferability of deep representation [1, 11, 37, 39]. We show that generative methods approach a better upper bound of $I(X; T)$, and introducing multiple generative objectives can further improve the upper bound of $I(X; T)$.

Empirical observations and theoretical analyses jointly inspire us to design the fourth paradigm, multi-modal generative pre-training. See Fig. 1 (iv). Under the paradigm, we propose a novel vision learner for web image-text data pre-training, named **M**U**L**ti-modal **G**enerator (MUG). MUG is purely composed of multi-modal generative objectives. The optimization objective of MUG is generating the multi-modal joint distribution with a single-modal image distribution. We show that MUG has a better upper bound for feature transferability from the information-theoretical view, which helps the vision encoder learn more transferable representations than previous paradigms. Empirical results on a variety of downstream tasks further validate the advantage of MUG on vision pre-training with web image-text paired data. Extensive ablations are provided to understand critical components. Visualizations are provided to prove that our learned representations can generate the joint distribution.

2. Related Work

Numerous vision learners have been proposed in recent years; we briefly review relevant techniques below.

2.1. Vision Learners with Contrastive Learning

Contrastive learning is a representative paradigm for self-supervised representation learning. The pretext is instance discrimination [49] which learns the representation by pulling positive examples from the augmentations of the same image closer and pushing negative examples from different images apart in the embedding space. MoCo [9, 10, 18] shows that by introducing more negative examples using a momentum encoder and memory bank, SimCLR [7, 8] shows that larger mini-batch size and stronger augmentations greatly benefit contrastive learning. A variety of tech-

niques for improving contrastive learning have been proposed, including hard example mining [25, 56], image mixture [36, 59], and injecting localized priors [20, 44, 47, 52]. The underlying principle of contrastive learning is the InfoMax principle [23] which indicates that the mutual information $I(X; T)$ between the input image X and the encoded representation T should be maximized so that the representation of one image can identify the only corresponding image in the whole dataset. In CTC [11], it has been proved that the mutual information $I(X; T)$ is the key to the transferability of one representation, alleviating the decrease of $I(X; T)$ during training can indeed improve the transferability of the learned representation. CTC [11] also shows that contrastive learning is learning to optimize $I(X; T) = H(T) - H(X|T)$ by increasing $H(T)$.

2.2. Vision Learners with Masked Image Modeling

Inspired by the success of masked language modeling (MLM) with transformers [43] for natural language processing [5, 14], masked image modeling [3, 6, 17, 53] has been proposed for learning representations with a vision transformer [15, 40], specifically, iGPT [6] learns the representation by predicting unknown pixels from a sequence of pixels, BEiT [3] propose to predict a set of discrete tokens from the encoder of DALLÉ [33, 41], the task is simplified by MAE [17] and SimMIM [53] which only enforces the model to reconstruct the masked pixels of the input image. The pretext of masked image modeling can be seen as to optimize for $-\log p(X|T)$ where T is the representation of the non-masked tokens and $p(X|T)$ is the likelihood of generating the masked image given the learned representation of the input tokens, this is equal to minimizing $H(X|T)$ and given that $I(X; T) = H(X) - H(X|T)$, we can see that masked image modeling still follows the InfoMax [23] principle where the optimization of $I(X; T)$ is done by optimizing $H(X|T)$ instead of $H(T)$ in contrastive learning. MIM has been proven more effective for learning transferrable representations than contrastive learning [17, 53], indicating the effectiveness of generative pretraining.

2.3. Vision Learners with Web Image-Text Pairs

It is relatively easy to collect a large-scale dataset of image-text paired data from the web [34, 35]; Many works studied to enhance the learned visual representations of the model with web image-text datasets [26, 27, 30, 32, 54, 55]. CLIP [32] tackles this challenge by performing contrastive learning over the paired image and text data. SLIP [30] learns the representation by joint performing contrastive learning on both image-text paired datasets and image-only datasets. CoCa [55] proposes to learn the representation by cross-modal contrastive learning and auto-regressive caption generation. In this work, we first comprehensively study these methods for learning transferrable representa-

tions on publicly available image-text paired datasets. We propose a new method for learning representations based on the insight from our benchmark.

3. Preliminary

3.1. Benchmarking SSL Methods on Web Data

Given a dataset of image-text pairs $\mathcal{D} = \{(x_i^V, x_i^L)\}$ sampled from the joint distribution of $p(X^V, X^L)$, where $x_i^V \in \mathbb{R}^{C \times H \times W}$, $x_i^L \in \mathbb{R}^{C \times L}$, our goal is to learn a visual feature encoder $f: \mathbb{R}^{C \times H \times W} \rightarrow \mathbb{R}^D$ that maps the input image into a compact feature embedding and enables good transfer learning performance [19].

Motivation. Two types of self-supervised learning methods can be used to achieve this goal. One is single-modal SSL using only the images x_i^V within the dataset \mathcal{D} . Sec. 2.1 and Sec. 2.2 introduce the most representative methods of single-modality SSL. The other is multi-modal SSL, aiming to learn a good representation by aligning the representation of the image input and the corresponding text input, and a brief introduction of multi-modal SSL methods is provided in Sec. 2.3. As a preliminary for our work, we first provide a benchmark study. We pre-train these SSL methods *on the same web image-text dataset with the same training epochs*. Then, we evaluate the transferring performance by fine-tuning pre-trained models.

Setting. We categorize methods according to pre-training manners, as discussed in Fig. 1. For single-modal SSL methods, we choose MoCoV3 [10], SimCLR [7] as discriminative ones, and MAE [17] as generative. For image-text multi-modal SSL, we choose CLIP [32] and SLIP [30] as discriminative ones. CoCa [55] is composed of both discriminative and generative targets. Notably, other than these methods, we further implement a multi-modal method, namely Masked Captioner (MAC), for generating texts with masked images. It only contains a cross-modal generative target. For pre-training hyper-parameters, we strictly follow the recommended setting in the original paper of each method. For a fair comparison, we pre-train all methods on a web dataset CC3M [35] for 400 epochs. When transferring the representation to ImageNet-1K [13], we follow the widely used fine-tuning recipe introduced by [3, 17].

3.2. Key Observations and Inspirations

We have the following key observations from Tab. 1:

Generative methods (e.g., MAE) achieve the best results. Comparing all methods, we can observe that MAE [17] achieves the best performance. As mentioned in Sec. 2.1 and Sec. 2.2, we argue that discriminative pre-training and generative pre-training are approaching the InfoMax [23] principle via different mechanisms, *i.e.*, discriminative pre-training optimizes $I(X; T_d) = H(T_d) - H(T_d|X)$ via maximizing $H(T_d)$ and generative pre-training opti-

method	pre-train manner	IN-1K [13]
<i>single-modal pre-training</i>		
MAE [17]	gen. \mathcal{I}	83.0
SimCLR [7]	disc. \mathcal{I}	82.7
MoCoV3 [10]	disc. \mathcal{I}	82.6
<i>multi-modal pre-training</i>		
MAC (impl.)	gen. \mathcal{T} w. \mathcal{I}	81.7
CLIP [32]	disc. $\mathcal{I} \& \mathcal{T}$	79.7
SLIP [30]	disc. $\mathcal{I} \& \mathcal{T}$ + disc. \mathcal{I}	80.9
CoCa [55]	disc. $\mathcal{I} \& \mathcal{T}$ + gen. \mathcal{T} w. \mathcal{I}	79.5

Table 1. Comparison of previous pre-training methods. All models are pre-trained on the CC3M [35], and evaluated on ImageNet-1K (IN-1K) [13] via end-to-end fine-tuning. “gen. and dist.” are short for generating and discriminating. “ \mathcal{I} and \mathcal{T} ” denote images and texts. For instance, SimCLR [7] is pre-trained by discriminating images (disc. \mathcal{I}). CLIP [32] is pre-trained by discriminating image-text pairs (disc. $\mathcal{I} \& \mathcal{T}$). CoCa [55] has two objectives: discriminating image-text pairs (disc. $\mathcal{I} \& \mathcal{T}$) and generating texts with images (gen. \mathcal{T} w. \mathcal{I}). Other than existing methods, we implement (impl.) a MAsked Captioner (MAC) to generate texts with masked image patches (gen. \mathcal{T} w. \mathcal{I}).

mizes $I(X; T_g) = H(X) - H(X|T_g)$ via minimizing $H(X|T_g)$ [11], where T_d is the representation learned by discriminative pre-training, and T_g is the representation learned by generative pre-training. Suppose the models learned by generative pre-training and discriminative pre-training both achieve zero training loss, then $I(X; T_d)$ will be $H(T_d)$ and $I(X; T_g)$ will be $H(X)$. In the discriminative pre-training scenario, consider the Markov Chain of $X \rightarrow T_d$, we have $I(X; X) \geq I(X; T_d)$ from the data process inequality, *i.e.*, $H(X) \geq I(X; T_d) = H(T_d)$, thus generative pre-training has a better transferability upper bound than discriminative pre-training, thus more informative and beneficial features for downstream tasks.

Present multi-modal methods cannot outperform single-modal ones. Comparing the single-modal and multi-modal methods, we can observe a large margin, *i.e.*, the best single-modal method outperforms the best multi-modal pre-training method by 1.3% on the ImageNet-1K accuracy. Compared with our introduced MAC, multi-modal discriminative methods yield worse results, *e.g.*, CLIP, and CoCa. We believe the reason is that *the information of text modality is greatly limited*. A typical text annotation contains partial information about the scene in the image, and Yann Lecun comments that “Language is a very low-bandwidth method for transmitting information: isolated words or sentences, shorn of context, convey little.”² It suggests the $H(X^L)$ could be much lower than $H(X^V)$. Regarding the multi-modal discriminative method CLIP, a low $H(X^L)$ directly limits $I(X^L; T_d)$; thus, bad transferring results are

²Discussed in the essay: AI and the Limits of Language.

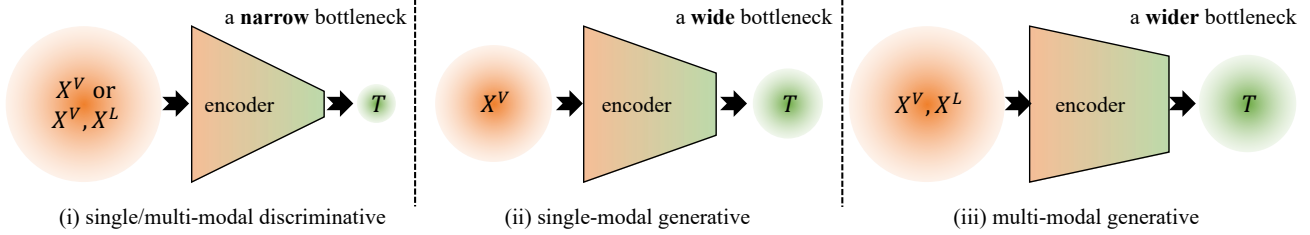


Figure 2. **Left:** Single/Multi-modal discriminative method has a narrow bottleneck and learns a less informative representation. **Middle:** Single-modal generative one has a wide bottleneck and learns an informative representation. **Right:** Multi-modal generative one has a wider bottleneck for generating (e.g., recovering) a joint distribution of both modalities, then learns a more informative representation.

obtained. Comparing SimCLR and SLIP, we observe that SLIP falls behind SimCLR by 1.8% accuracy, which further proves the side effect of multi-modal discriminative objectives. However, MAC is generative and alleviates this problem, but it still cannot outperform single-modal methods.

Discussions and inspirations. Inspired by the information-bottleneck theory [1, 11, 23, 37, 39], we provide an illustration to understand our observations in Fig. 2. The first inspiration is that generative methods can help the model learn more transferable visual representations than discriminative ones due to a better $I(X; T)$ upper bound. In Fig. 2 (left), we argue that discriminative methods have a narrow bottleneck and a low $I(X; T)$, thus a less informative representation.³ In Fig. 2 (middle), generative ones have a wide bottleneck, leading to a more informative representation. Considering the side effects of multi-modal discriminative objectives (the second inspiration), developing multiple generative objectives will force the model to learn informative representations. As shown in Fig. 2 (right), for image-text pair, generating the joint distribution of both image and text modality will help the model to “absorb” as much information as possible from the data and approach a large $I(X; T)$.

4. Approach

4.1. Motivation

Following the above observations and inspirations, we attempt to learn a better vision encoder based on web image-text paired data. We will first formulate the mechanism that a multi-modal generative objective helps to learn a better transferable representation, in line with Fig. 2 (right). We believe that introducing multiple generative objectives is feasible, and the optimization objective becomes to learn to generate the joint distribution $p(X^V, X^L)$ from a single distribution X^V since we focus on learning visual encoders.

For generating a joint distribution $p(X^V, X^L)$ from latent representation $T = f(\hat{X}^V)$ extracted from the visual input, the model is maximizing the following mutual infor-

mation:

$$\begin{aligned}
 I(X^V, X^L; T) &= H(X^V, X^L) - H(X^V, X^L|T) \\
 &\geq \max [H(X^V), H(X^L)] - \\
 &\quad H(X^V, X^L|T).
 \end{aligned} \tag{1}$$

Consider the model is fully optimized to the optimal, thus $H(X^V, X^L|T) = 0$. Because the lower bound of $I(X^V, X^L; T)$ is greater than or equal to the lower bound of $I(X^V; T)$, we can see that generating the joint distribution of $p(X^V, X^L)$ can at least learn an equally transferable representation as single-modal generative pre-training. In practice, we observe that the multi-modal generative pre-training achieves superior transferability. This design motivation is also in line with discussions in Sec. 3.2. Overall this is a generative pre-training framework with multiple generation tasks relying on learned visual representations.

4.2. MUG: Multi-modal Generator

Then, we design a novel multi-modal generative vision learner, namely MUlti-modal Generator (MUG). The framework of MUG is presented in Fig. 3, consisting of an image encoder, an image decoder, and a text decoder. All modules are based on Transformer layers. Two tasks are involved, *i.e.*, raw pixel and original caption generation.

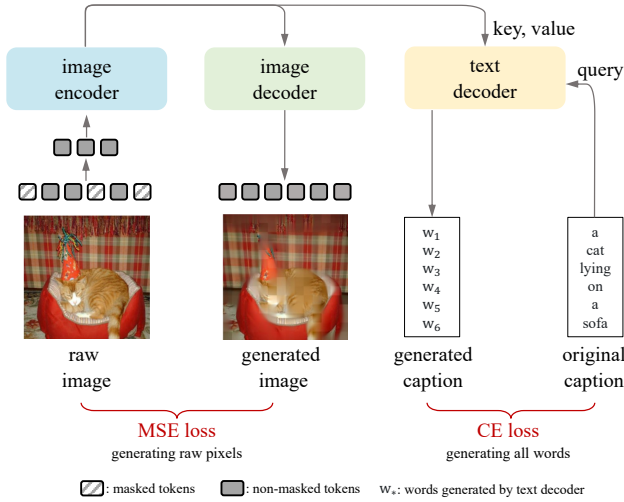
Raw pixel generation. Given a masked visual input $\hat{x}_i^V = M \odot x_i^V$ where M is the random generated 0-1 mask following the procedure in MAE [17] and \odot denotes the elementwise product, the feature encoder f maps this input to a latent representation $t_i^V = f(\hat{x}_i^V)$. The latent representation t_i^V is then fed into a visual decoder g_V to generate $\tilde{x}_i^V = g_V(t_i^V)$ which is the reconstruction of the non-masked visual input. We adopted the reconstruction loss from MAE [17] to train both f and g_V :

$$\mathcal{L}_V = \frac{1}{\Omega(\hat{x}_i^V)} \|(1 - M) \odot x_i^V - (1 - M) \odot \tilde{x}_i^V\|^2, \tag{2}$$

where $\Omega(\hat{x}_i^V)$ is the number of masked elements in \hat{x}_i^V . This loss generates the visual part of the input.

Caption generation. We further propose to generate the coupling caption x_i^L by the feature t_i^V of the masked visual

³More detailed discussions are attached in Appendix A.2.



Algorithm 1 Pseudocode of MUG .

```

# img, txt: image-text paired data
# txt_mask: causal mask for captioning
def text_decoder(q, kv, mask):
    q = unimodal_attn(q, mask)
    cap_res = multimodal_attn(q, kv)
    return cap_res

patch_img = patchify(img)
masked_token = masking(patch_img) # [N, L, D]
latent = vit_encoder(masked_token) # [N, L, D]

# Generative objective for visual
recon_img = mae_decoder(latent) # [N, L, D]
recon_loss = mse_loss(img, recon_img)

# Generative objective for text
label, txt = txt[:, 1:, :], txt[:, :-1, :]
txt_feat = tokenizer(txt) # [N, L, D]
cap_res = text_decoder(q=txt_feat, kv=latent, mask=
    txt_mask)
cap_loss = ce_loss(label, cap_res)

```

Figure 3. Illustration and the pseudo-code of MUG . The input image is masked and fed into the image encoder, and then the resulting latent representation will be used by an image decoder and a text decoder. The image decoder enables the training objective of generative the raw pixels of the image, and the text decoder enables the training objective of generating the paired caption of the input image..

input \hat{x}_i^V . To do this, we fed the feature t_i^V to a text decoder g_L to generate the textual captions $\tilde{x}_{i,j}^L = g_L(x_{i,<j}^L, t_i^V)$ in an auto-regressive fashion, driven by the following loss:

$$\mathcal{L}_L = - \sum_{j=1}^J \log P(\tilde{x}_{i,j}^L | x_{i,<j}^L, t_i^V), \quad (3)$$

where J is the maximum length of a textual caption. We aim to drive the text generation by image features, which helps to improve the transferability of the image encoder. Thus, the proposed text decoder has two parts, *i.e.*, uni-modal and multi-modal layers. The uni-modal part is constructed as an auto-regressive model via a causal mask [43], where each word can only attend to the words before itself in a caption sequence. It only provides the text decoder with contextual information when generating the caption. We design the multi-modal part using the image features as the *key* and *value* and the output from uni-modal layers as the *query* in cross-attention learning. It ensures the text generation derives from image features since contextual information only serves as the *query*. Thus, the entire text decoder can be seen as regrouping the image features t_i^V with contextual information to generate captions.

Optimization. Our joint multi-modal pre-training framework simultaneously optimizes the above two losses:

$$\mathcal{L} = \lambda_V \mathcal{L}_V + \lambda_L \mathcal{L}_L, \quad (4)$$

where λ_V and λ_L are different weights for image reconstruction and text generation tasks.

4.3. Understanding the Loss Function

If we consider each natural image as a Gaussian distribution, then the loss in Eq. (2) is actually maximizing the

log-likelihood of the generated image:

$$\begin{aligned} \log P_{x_i^V}(\tilde{x}_i^V) &= \log \frac{1}{\sigma\sqrt{2\pi}} \exp\left(-\frac{1}{2} \left(\frac{\tilde{x}_i^V - x_i^V}{\sigma}\right)^2\right) \\ &= -\frac{1}{Z} \|\tilde{x}_i^V - x_i^V\|^2 - C, \end{aligned} \quad (5)$$

where σ is the standard deviation of distribution. Z and C are constants that do not affect the optimization process. Together with \mathcal{L}_L , we can see that our loss function in Eq. (4) is maximizing the log-likelihood of both the generated image and the generated textual caption. Thus the latent representation T extracted by the model optimized to be more predictive of the image X^V and the caption X^L . In other words, the conditional entropy $H(X^V, X^L | T)$ is minimized via the two losses in our framework, maximizing the mutual information $I(X^V, X^L; T)$ and leading to a more transferrable representation.

5. Experiment

5.1. Implementation Details

Encoders and decoders. Our framework contains an image encoder f , and two decoders g_V and g_L for decoding the latent representation to reconstruct the image and the textual caption, respectively. The image encoder f is implemented as Vision Transformer [15] backbone, and the image decoder is implemented with the same architecture as in MAE [17]. We follow SimVLM [45] to implement the text decoder g_L . We train this encoder-decoder architecture with teacher-forcing [48] to learn the model efficiently.

Pre-training datasets. We train the models on the publicly available CC3M dataset [35]. Other than CC3M, we also

collect 200M web image-text pairs to study the scalability of MUG. The collected data has no filtering processing and tremendous noises could be contained, presenting a challenge for MUG. We name the privately collected dataset as W200M in the following.

5.2. Transfer Learning

In this part, we transfer learned representations to a wide range of downstream tasks, proving the superiority of MUG to previous pre-training methods.

General image classification on ImageNet-1K. First, we transfer learned representations to general image classification on ImageNet-1K with end-to-end fine-tuning. Other than the original images in ImageNet-1K, we also evaluate fine-tuned models on out-of-distribution datasets ImageNet-Adversarial (IN-A) [22] and ImageNet-Rendition (IN-R) [21]. Results are reported in Tab. 2 and Tab. 3. Compared to previous methods, MUG achieves the best top-1 accuracy 83.5% (with CC3M) and 83.7% (with W200M). When training MUG with ViT-S, ViT-B, and ViT-L backbones, consistent improvements are achieved over the previous state-of-the-art method MAE. Both comparisons prove that MUG surpasses previous methods with scalable web image-text pairs. For results on IN-A and IN-R, MUG also outperforms previous methods, which indicates the robustness of MUG’s representation.

method	data	#epoch	IN-1K	IN-A	IN-R
<i>single-modal pre-training</i>					
SimCLR	CC3M	400	82.7	31.2	49.1
MoCoV3	CC3M	400	82.6	29.7	46.9
MAE	CC3M	400	83.0	32.9	49.4
<i>multi-modal pre-training</i>					
CLIP	CC3M	400	79.7	23.6	42.6
SLIP	CC3M	400	80.5	20.5	44.4
CoCa	CC3M	400	79.5	18.1	42.9
MAC (impl.)	CC3M	400	81.7	27.5	44.3
MUG (ours)	CC3M	400	83.5	36.3	50.4
MAE*	IN-1K	1600	83.6	35.9	48.3
MAE†	W200M	10	83.3	35.3	50.4
MUG†(ours)	W200M	10	83.7	39.0	51.8

Table 2. Comparison of pre-training methods on ImageNet-1K (IN-1K) fine-tuning, and top-1 accuracies are reported. Besides, we evaluated fine-tuned models on ImageNet-Adversarial (IN-A) and ImageNet-Rendition (IN-R) for evaluating out-of-distribution performances. † means the model is pre-trained with our collected 200M web image-text pairs. MAE* is pre-trained on IN-1K.

Second, we evaluate pre-trained models with linear probing tasks on ImageNet-1K. Results are reported in Tab. 4 and Tab. 5. MUG still suffers from unsatisfactory linear probing results, similar to conclusions in MAE [17]. Com-

method	backbone	IN-1K	IN-A	IN-R
MAE	ViT-S	80.9	22.7	44.1
MUG (ours)	ViT-S	81.6	25.0	42.5
MAE	ViT-B	83.0	32.9	49.4
MUG (ours)	ViT-B	83.5	36.3	50.4
MAE	ViT-L	85.0	49.4	59.6
MUG (ours)	ViT-L	85.4	53.8	63.1

Table 3. Comparison of different backbone sizes, which are pre-trained with CC3M for 400 epochs and fine-tuned on IN-1K. Accuracies of ViT-S, ViT-B, and ViT-L are reported.

pared with discriminative pre-training methods, most generative methods are all unsatisfactory. For instance, SimCLR and MUG achieve 63.3% and 61.3%, respectively. It could result from that linear probing requires discriminative representations, which cannot be satisfied by generative methods. However, compared with the original MAE, MUG outperforms the original MAE by large margins. Notably, with the backbone ViT-S, our method outperforms MAE by **11.3%** top-1 accuracy. It indicates that MAE pre-trained models could suffer from poor results due to low model capacities, and MUG pre-trained models could alleviate the drawback with the help of external data information from the text modality. Interestingly, we observe that the MUG model pre-trained on 200M in-house data would achieve comparable results with the MAE model pre-trained on ImageNet-1K. The result proves that, with scaling annotation-free web data, MUG learns greatly transferable and linearly separable representations.

	single-modal	SimCLR	MoCoV3	MAE	MAE*	MAE†
lp. top1-acc.		63.3	61.6	57.4	68.0	53.8
	multi-modal	CLIP	SLIP	CoCa	MUG	MUG†
lp. top1-acc.		55.1	55.2	56.9	61.3	68.0

Table 4. Comparison of single/multi-modal pre-training methods on IN-1K linear probing (lp.), and top-1 accuracies are reported.

method	ViT-S	ViT-B	ViT-L
MAE [17]	41.0	57.4	63.5
MUG (ours)	52.3	61.3	67.6

Table 5. Comparison of different backbone sizes. Models are pre-trained with CC3M for 400 epochs and evaluated with linear probing on IN-1K. We evaluate the ViT-S, ViT-B, and ViT-L.

Fine-grained image classification. To prove that our pre-trained models do not “over-fit on ImageNet-1K evaluations”, we further transfer learned representations to fine-grained image datasets iNaturalist-17 (iNat-17) [42], iNaturalist-18 (iNat-18), and Places365-Small (P365) [57] with end-to-end fine-tuning. Results are reported in Tab. 6.

Similar to the results of ImageNet-1K, MUG still outperforms the previous SOTA method MAE on all evaluated cases. It further validates the success and robustness of MUG in transferring to image classification tasks. Moreover, we notice that the performance of MUG is relevant to the pre-training data domain. Concretely, iNat-17 and iNat-18 share a similar domain with IN-1K; thus, the IN-1K MAE models perform better than CC3M MAE models. P365 shares a similar domain with CC3M, which leads to better results of CC3M-based models. Regardless of the fine-tuning data domain, MUG’s improvements are stable and generalizable.

method	backbone	iNat-17	iNat-18	P365
MAE	ViT-S	65.4	70.0	57.9
MUG (ours)	ViT-S	65.5	70.7	58.3
MAE*	ViT-B	70.5	75.4	57.9
MAE	ViT-B	67.9	73.0	58.3
MUG (ours)	ViT-B	68.4	73.4	58.6
MAE†	ViT-B	68.1	73.7	58.9
MUG†(ours)	ViT-B	70.7	75.1	59.3
MAE	ViT-L	73.0	76.8	59.4
MUG (ours)	ViT-L	75.1	77.8	59.8

Table 6. Comparison of pre-training methods on fine-grained iNaturalist-17 (iNat-17), iNaturalist-18 (iNat-18), and Places365 (P365) fine-tuning. Top-1 accuracies are reported. † means the model is pre-trained with our collected 200M web image-text pairs. MAE* is pre-trained on IN-1K.

Semantic segmentation on ADE20K. We transfer MUG to the semantic segmentation task on the ADE20K dataset [58]. Experiments on ADE20K are based on the UperNet [50] decode head, and training recipes follow the default setting provided in `mmsegmentation`, where training resolution is set to 512×512 , and the number of iterations is 160k. We evaluate models with different capacities, as reported in Tab. 7. It shows that our MUG significantly improves the transferring results on ViT-S, ViT-B, and ViT-L. We can observe that ViT-S MAE model only achieves 40.7% mIoU, which is similar to IN-1K linear probing results. MUG significantly alleviates the performance drop on the small backbone by improving 2.6% mIoU. Besides, compared to CLIP and MoCoV3, the superiority of MUG could support our information-theoretical motivations, *i.e.*, generative pre-training has a better transferability upper bound than discriminative pre-training. Consequently, generative pre-training can greatly benefit downstream fine-tuning tasks.

5.3. Extension Experiments

Ablation: Effects of image reconstruction and text generation tasks. The most important ablation is the trade-off between the image reconstruction loss weight λ_V and the

method	backbone	data	#epoch	mIoU
MAE	ViT-S	CC3M	400	40.7
MUG (ours)	ViT-S	CC3M	400	43.3
CLIP	ViT-B	CC3M	400	39.4
SLIP	ViT-B	CC3M	400	38.1
MoCoV3	ViT-B	CC3M	400	46.5
MAE	ViT-B	CC3M	400	45.5
MUG (ours)	ViT-B	CC3M	400	47.5
MoCoV3*	ViT-B	IN-1K	1600	47.3
MAE*	ViT-B	IN-1K	1600	48.1
MAE†	ViT-B	W200M	10	46.3
MUG†(ours)	ViT-B	W200M	10	48.5
MAE	ViT-L	CC3M	400	50.0
MUG (ours)	ViT-L	CC3M	400	52.1

Table 7. Comparison of pre-training methods on ADE20K semantic segmentation fine-tuning, and mIoU scores are reported. † means the model is pre-trained with our collected 200M web data. MoCoV3* and MAE* are pre-trained on IN-1K.

caption generation loss λ_L . We fix the weight λ_V and ablate the value of λ_L . Evaluations are based on IN-1K fine-tuning experiments, and results are reported in Tab. 8. As reflected, the best transferring result is achieved by $\lambda_L = 0.1$, and both larger and smaller values perform worse. It reveals a trade-off between image reconstruction and text generation, and we attempt to explain the trade-off in the following. Setting $\lambda_L = 0.0$ degrades MUG to MAE, and it achieves inferior results because the pre-training data is composed of noisy images. Increasing λ_L in the range of (0.0, 0.3] increases the transferring results, showing the effectiveness of our introduced text generation task. Reasons for performance drops are two-fold: (i) Considering the pre-training data is web collected, increasing λ_L would emphasize a noisy text generation task, since the captions coupled with web images could be greatly irrelevant, *e.g.*, an image contains a river but its caption maybe about hiking. (ii) As discussed in Sec. 3.2, the information of text modality is greatly limited. Increasing λ_L unavoidably leads to the over-fitting problem, which is unfavorable in representation learning. Therefore, a trade-off between image reconstruction and text generation exists.

We further study the effects of the image reconstruction target. We simply set λ_V to 0.0 and set $\lambda_L = 1.0$, which only permits the text generation task. Interestingly, setting λ_V to 0.0 degrades MUG to MAC. Results are reported in the following table, and a notable performance drop is observed. It validates (1) the information of text modality is insufficient, and (2) the necessity of image generation for visual representation learning with image-text pairs.

λ_L	0.0	0.05	0.1	0.2	0.3	w/o λ_V	w/ λ_V
ft. top-1 acc.	83.0	83.3	83.5	83.2	83.0	81.7	83.5

Table 8. Ablation studies on loss weights.

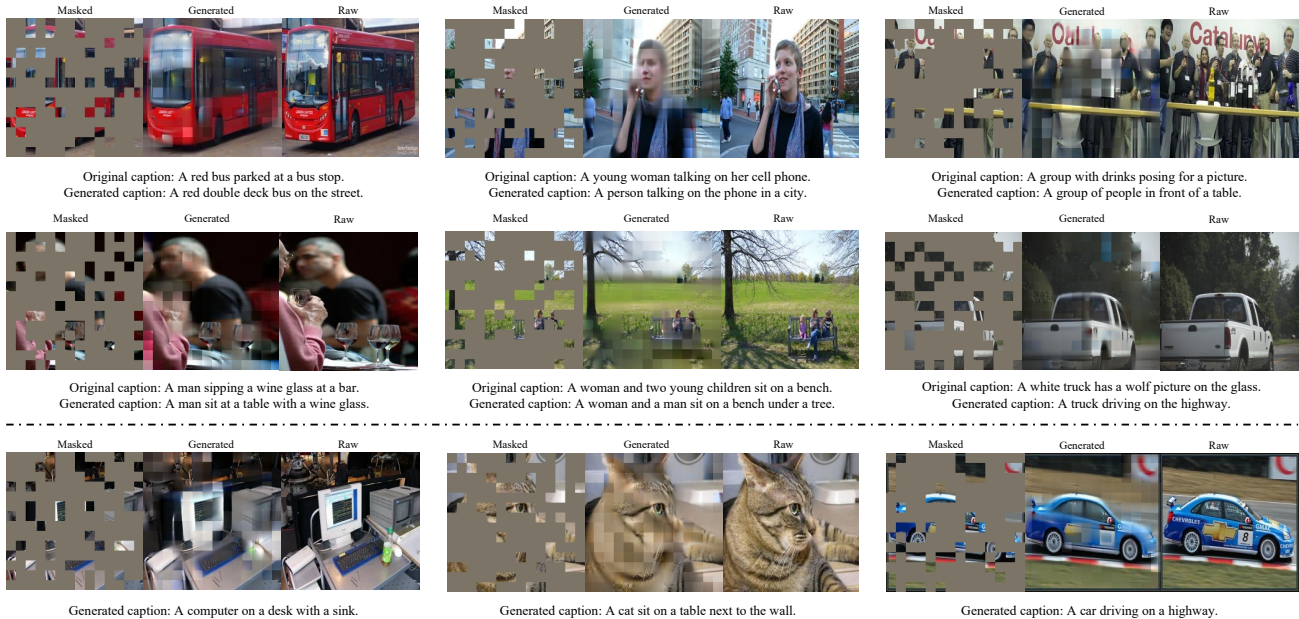


Figure 4. Reconstruction of masked images and captions on the MS-COCO (upper) and PASCAL-VOC (bottom) datasets.

Ablation: Effects of the number of layers in text encoder. Regarding the text generation task, both uni-modal and multi-modal layers are involved. We set the total number of layers to 10, and grid search for the best result, as reported in Tab. 9. We observe that setting the number of uni-layers to 1 or 2 achieves comparable results; however, when the number of multi-layers decreases to 6 and 5, the performance drops are significant. Discussions are two-fold: (i) A few uni-modal layers can support the text generation task since the uni-modal layers could serve as a key entity word extractor, which has a subtle influence on visual representation learning. (ii) A certain number of multi-modal layers could be required to support the text generation task. Inadequate multi-modal layers further hurt the learning of image reconstruction because the performances become lower than an MAE baseline (83.0%).

#uni-/#multi-layers	1/9	2/8	3/7	4/6	5/5
ft. top-1 acc.	83.3	83.5	83.0	82.5	82.1

Table 9. Ablation studies on textual layers.

Ablation: Effects of text generation task. We provide the ablation of text generation manners. There are two manners for text generation, *i.e.*, masked language modeling (MLM) and auto-regressive modeling (captioning). We set optimal λ_L values for both manners, and captioning outperforms MLM by 0.5% top-1 accuracy (83.5% vs. 83.0%). From the perspective of task property, *i.e.*, captioning is regularized to sequentially predict words while MLM is not regularized. A harder task could help to approach a higher $I(X^V, X^L; T)$. From another aspect, the text generator is composed of uni-modal and cross-modal parts, and the text generation man-

ner actually affects the learning mechanism of uni-modal part. Concretely, the auto-regressive learning target would force the uni-modal encoder to extract key words, *e.g.*, the word after an article could be a key entity noun. For masked language modeling, contextual words are possibly masked and predicted; however, such noisy and meaningless reconstruction tasks hardly benefit vision encoders.

Visualization: Reconstructed images and coupled texts. In Fig. 4, we provide generated images and captions produced by MUG on the MS-COCO [28] and PASCAL-VOC datasets [16]. Note that PASCAL does not provide captions. The input of MUG only consists of a masked image and a start word (*e.g.*, “a”). As observed, MUG can recover the main objects and entities in the raw images and annotated captions, even if the most image pixels are masked. It is reasonable that MUG only describes visible pixels, *e.g.*, in the middle of the second row, the left child is masked, and thus MUG only describes “a woman and a man”. The visualizations prove that the representation learned by MUG can generate the joint distribution $p(X^V, X^L)$.

6. Conclusion

In this paper, we first benchmark different self-supervised representation learning methods and obtain two observations: (i) Generative pre-training achieves the best transfer performance on web datasets, and (ii) multi-modal methods cannot outperform single-modal ones. An information-theoretical view is developed to understand the benchmarking results and our observations. The view further inspires us to propose a new vision learner based on

web image-text paired data, namely MULTI-modal Generator (MUG). MUG adopts the visual latent representations for two generative objectives. MUG shows strong generalizability on several transfer learning tasks and satisfactory scaling results, validating our information-theoretical view.

A. Appendix

A.1. Implementation Details

Pre-training. The default setting is in Tab. 10, and hyperparameters mainly follow [17] for fair comparisons. For each caption, we set the max length to 70 and use a percentage of 20% input words for processing. For each word, we mask it, replace it with a random word, or delete it with a probability of 50%, 10%, and 40%, respectively.

End-to-end fine-tuning in IN-1K, iNat-17, iNat-18, and P365. We fine-tune models with the widely used recipe [3, 17] in Tab. 11 except for the layer-wise decay rate is set to 0.7. On all evaluated datasets and pre-training models, we use the same setting for fair comparisons.

Linear probing. Settings are provided in Tab. 12. We follow [17] to introduce an extra BatchNorm layer without affine transformation for improving linear probing performances. For fair comparisons, all evaluated models are equipped with the extra layer.

Semantic segmentation in ADE20K. The ADE20K fine-tuning setting can be found in this [website](#). We advise settings for ViT-S and ViT-L by following [40] and [3], respectively. All evaluated pre-training models are fine-tuned with the same setting, and thus comparisons are fair.

config	value
optimizer	AdamW [29]
base learning rate	1.5e-4
weight decay	0.05
optimizer momentum	$\beta_1, \beta_2=0.9, 0.95$
batch size	4096
learning rate schedule	cosine decay
warmup epochs	40
image augmentation	RandomResizedCrop
text augmentation	mask/replace/delete
λ_V	1.0
λ_L	0.1

Table 10. **Pre-training setting.**

A.2. Further Discussions on the Information Bottleneck View

In Sec. 3.2, we discussed about the inspirations of preliminary benchmark experiments. In this part, we extend the discussion from the following perspectives:

config	value
optimizer	AdamW
base learning rate	1e-3
weight decay	0.05
optimizer momentum	$\beta_1, \beta_2=0.9, 0.999$
layer-wise lr decay	0.7
batch size	1024
learning rate schedule	cosine decay
warmup epochs	5
training epochs	100 (B), 50 (L)
augmentation	RandAug (9, 0.5)
label smoothing	0.1
mixup	0.8
cutmix	1.0
drop path	0.1

Table 11. **End-to-end fine-tuning setting.**

config	value
optimizer	LARS
base learning rate	0.1
weight decay	0
optimizer momentum	0.9
batch size	16384
learning rate schedule	cosine decay
warmup epochs	10
training epochs	90
augmentation	RandomResizedCrop

Table 12. **Linear probing setting.**

Why does the single/multi-modal discriminative method have a narrow bottleneck? Since popular discriminative methods are based on the contrastive learning, the nature of such methods could be regarded as the few-shot classification task, and the reason is as follows. In each batch, we can regard each sample as a category, and the few-shot learning setting is B-way 1-shot, where B represents the batch size. For instance, in SimCLR [7], an image is processed by two data augmentations as a positive pair, and “pulling close” the positive pair is actually minimizing a classification loss, *i.e.*, the cross entropy loss. We believe the information compression rate of a classification task is relatively large, since the model only requires the most representative patterns to distinguish defined categories. Information irrelevant to the classification task will be compressed in the training process. Therefore, regarding discriminative methods as classification tasks would explain the narrow information bottleneck, and thus the $I(X; T_d)$ would be relatively small because of significantly compressed input information. In addition, it also explains that contrastive learning pre-training methods require a large batch size [12], since increasing batch size will increase the difficulty of the few-shot classification task, which further alleviates the information compression. The narrow bottleneck also suggests that such methods require a certain amount of pre-training data, and insufficient data could result in the over-fitting problem.

Why does the single-modal generative method have a wide bottleneck? Popular single-modal generative meth-

ods are based on masked image modeling in an encoder-decoder fashion, and the working mechanism of such methods could be regarded as the image reconstruction task. The image reconstruction task is much more challenging than the contrastive learning (or few-shot classification) task, because the model is driven to preserve as much information as possible for recovering details (concrete pixel values) in the raw input image. It explains the wide bottleneck, since the decoder cannot finish the reconstruction task without sufficient information of the encoder’s output. Thus, the $I(X; T_g)$ would be larger than $I(X; T_d)$, and the upper bound is $H(X)$. Therefore, better transferring results are achieved [3, 17, 31] by using single-modal generative methods than discriminative methods. The wide bottleneck also explains that generative methods can still perform well with a relatively small amount of pre-training data, as proven in [17].

Why does the multi-modal generative method have a wider bottleneck? This work requires the model to reconstruct the raw input image and the coupled caption. It drives the model to preserve more information than the single-modal generative methods, since two objectives are involved and the decoder generates a joint distribution $p(X^V, X^L)$. The information bottleneck of a multi-modal generative method can be wider than that of a single-modal generative one. In this way, we drive the $I(X; T)$ to approach $H(X^V, X^L)$, which has the potential to learn more transferable representations.

How about scaling pre-training data? Note that the above discussions are based on a hypothesis that the pre-training data is fixed, e.g., CC3M in this work. Moreover, results in Sec. 5 prove that the transferring results of our proposed multi-modal generative method are the best. We further discuss the choice of pre-training methods when the pre-training data is scalable.

As aforementioned, single-modal discriminative methods could suffer from a large information compression rate; however, we can increase the amount of pre-training data as compensation. To prove this, we pre-train the SimCLR [7] with our collected W200M data, and then we transfer the model via ImageNet-1K end-to-end fine-tuning. MAE (with W200M) and SimCLR (with W200M) achieve 83.3% and 83.4% top-1 accuracies, respectively. It means that, with large-scale data, the drawback of single-modal discriminative methods could be overcome. Besides, it also suggests that the scalability of single-modal generative methods can be inferior. However, our method MUG has good scalability by achieving 83.7%. Therefore, we suppose that our proposed method can perform well on different scales of pre-training data, which is an additional advantage.

A.3. More Visualization Results

We further provide visualizations of the reconstructed images as well as the generated captions produced by our model on randomly selected images on the MS-COCO and PASCAL-VOC datasets in Figs. 5 and 6 for qualitatively understand the model’s behaviour.

A.4. Limitations and Border Impact

One common limitation of models pre-trained on web-based image-text pairs is that the models will inevitably be influenced by the open nature of the internet contents, such as biases or hate speech; thus the models may learn unwanted behaviors that may cause actual harm to people. Given this limitation, the model should be tested thoroughly before it is deployed in real-world applications.

References

- [1] Alexander A Alemi, Ian Fischer, Joshua V Dillon, and Kevin Murphy. Deep variational information bottleneck. In *ICLR*, 2017. 2, 4
- [2] Alexei Baevski, Wei-Ning Hsu, Qiantong Xu, Arun Babu, Jiatuo Gu, and Michael Auli. Data2vec: A general framework for self-supervised learning in speech, vision and language. In *ICML*, 2022. 1
- [3] Hangbo Bao, Li Dong, and Furu Wei. BEiT: BERT pre-training of image transformers. In *ICLR*, 2022. 1, 2, 3, 9, 10
- [4] Adrien Bardes, Jean Ponce, and Yann LeCun. Vi-creg: Variance-invariance-covariance regularization for self-supervised learning. In *ICLR*, 2022. 1
- [5] Tom B. Brown, Benjamin Mann, Nick Ryder, Melanie Subbiah, Jared Kaplan, Prafulla Dhariwal, Arvind Neelakantan, Pranav Shyam, Girish Sastry, Amanda Askell, Sandhini Agarwal, Ariel Herbert-Voss, Gretchen Krueger, Tom Henighan, Rewon Child, Aditya Ramesh, Daniel M. Ziegler, Jeffrey Wu, Clemens Winter, Christopher Hesse, Mark Chen, Eric Sigler, Mateusz Litwin, Scott Gray, Benjamin Chess, Jack Clark, Christopher Berner, Sam McCandlish, Alec Radford, Ilya Sutskever, and Dario Amodei. Language models are few-shot learners. In *NeurIPS*, 2020. 2
- [6] Mark Chen, Alec Radford, Rewon Child, Jeffrey Wu, Heewoo Jun, David Luan, and Ilya Sutskever. Generative pre-training from pixels. In *ICML*, 2020. 2
- [7] Ting Chen, Simon Kornblith, Mohammad Norouzi, and Geoffrey Hinton. A simple framework for contrastive learning of visual representations. In *ICML*, 2020. 1, 2, 3, 9, 10
- [8] Ting Chen, Simon Kornblith, Kevin Swersky, Mohammad Norouzi, and Geoffrey Hinton. Big self-supervised models are strong semi-supervised learners. In *NeurIPS*, 2020. 1, 2
- [9] Xinlei Chen, Haoqi Fan, Ross Girshick, and Kaiming He. Improved baselines with momentum contrastive learning. *arXiv:2003.04297*, 2020. 1, 2
- [10] Xinlei Chen*, Saining Xie*, and Kaiming He. An empirical study of training self-supervised vision transformers. *arXiv:2104.02057*, 2021. 1, 2, 3

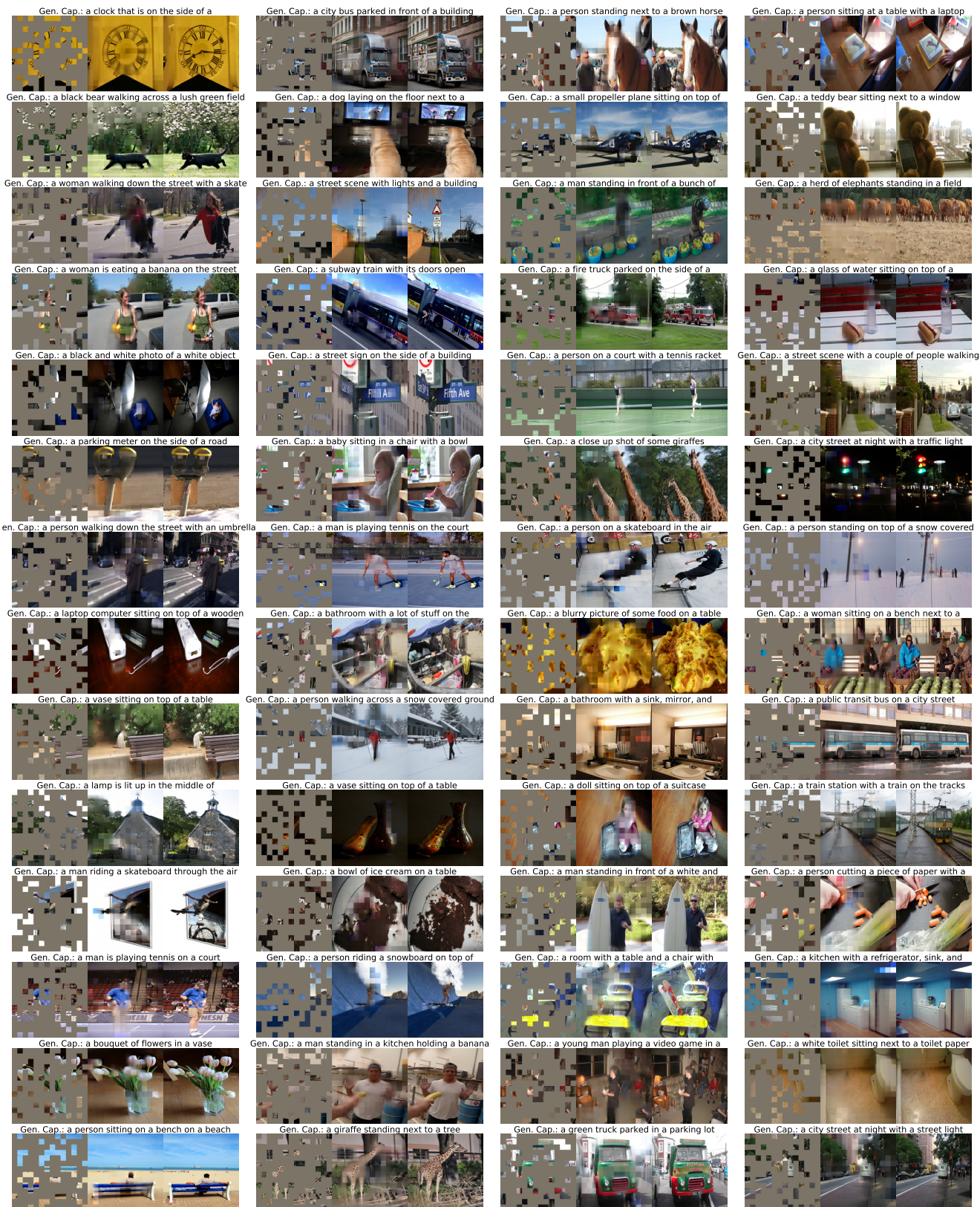


Figure 5. **Uncurated random samples** on COCO images. For each triplet, we show the masked image (left), MUG reconstruction (middle), the ground-truth (right), and the generated captions by MUG. The masking ratio is 75%.

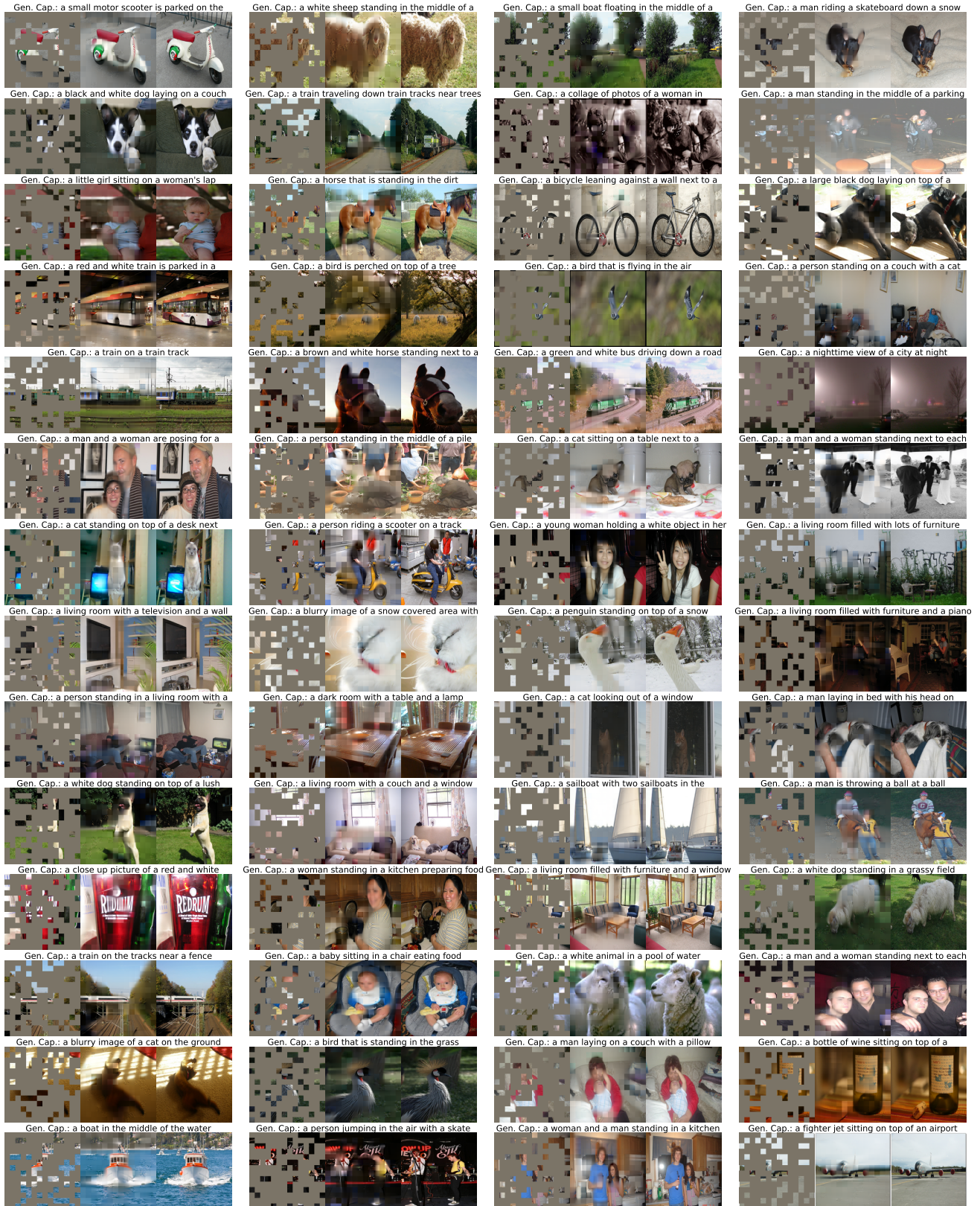


Figure 6. **Uncurated random samples** on PASCAL-VOC images. For each triplet, we show the masked image (left), MUG reconstruction (middle), the ground-truth (right), and the generated captions by MUG . The masking ratio is 75%.

- [11] Quan Cui, Bingchen Zhao, Zhao-Min Chen, Borui Zhao, Renjie Song, Jiajun Liang, Boyan Zhou, and Osamu Yoshie. Discriminability-transferability trade-off: An information-theoretic perspective. In *ECCV*, 2022. 2, 3, 4
- [12] Quan Cui, Boyan Zhou, Yu Guo, Weidong Yin, Hao Wu, Osamu Yoshie, and Yubo Chen. Contrastive vision-language pre-training with limited resources. In *ECCV*, 2022. 9
- [13] Jia Deng, Wei Dong, Richard Socher, Li-Jia Li, Kai Li, and Li Fei-Fei. Imagenet: A large-scale hierarchical image database. In *CVPR*, 2009. 1, 3
- [14] Jacob Devlin, Ming-Wei Chang, Kenton Lee, and Kristina N. Toutanova. Bert: Pre-training of deep bidirectional transformers for language understanding. In *NAACL*, 2018. 2
- [15] Alexey Dosovitskiy, Lucas Beyer, Alexander Kolesnikov, Dirk Weissenborn, Xiaohua Zhai, Thomas Unterthiner, Mostafa Dehghani, Matthias Minderer, Georg Heigold, Sylvain Gelly, Jakob Uszkoreit, and Neil Houlsby. An image is worth 16x16 words: Transformers for image recognition at scale. In *ICLR*, 2021. 2, 5
- [16] Mark Everingham, SM Eslami, Luc Van Gool, Christopher KI Williams, John Winn, and Andrew Zisserman. The pascal visual object classes challenge: A retrospective. *IJCV*, 2015. 8
- [17] Kaiming He, Xinlei Chen, Saining Xie, Yanghao Li, Piotr Dollár, and Ross Girshick. Masked autoencoders are scalable vision learners. In *CVPR*, 2022. 1, 2, 3, 4, 5, 6, 9, 10
- [18] Kaiming He, Haoqi Fan, Yuxin Wu, Saining Xie, and Ross Girshick. Momentum contrast for unsupervised visual representation learning. In *CVPR*, 2020. 1, 2
- [19] Kaiming He, Ross Girshick, and Piotr Dollár. Rethinking imagenet pre-training. In *ICCV*, 2019. 3
- [20] Olivier J Hénaff, Skanda Koppula, Jean-Baptiste Alayrac, Aaron van den Oord, Oriol Vinyals, and João Carreira. Efficient Visual Pretraining with Contrastive Detection. In *ICCV*, 2021. 2
- [21] Dan Hendrycks, Steven Basart, Norman Mu, Saurav Kadavath, Frank Wang, Evan Dorundo, Rahul Desai, Tyler Zhu, Samyak Parajuli, Mike Guo, et al. The many faces of robustness: A critical analysis of out-of-distribution generalization. In *CVPR*, 2021. 6
- [22] Dan Hendrycks, Kevin Zhao, Steven Basart, Jacob Steinhardt, and Dawn Song. Natural adversarial examples. In *CVPR*, 2021. 6
- [23] R Devon Hjelm, Alex Fedorov, Samuel Lavoie-Marchildon, Karan Grewal, Phil Bachman, Adam Trischler, and Yoshua Bengio. Learning deep representations by mutual information estimation and maximization. In *ICLR*, 2018. 1, 2, 3, 4
- [24] Chao Jia, Yinfei Yang, Ye Xia, Yi-Ting Chen, Zarana Parekh, Hieu Pham, Quoc V. Le, Yunhsuan Sung, Zhen Li, and Tom Duerig. Scaling up visual and vision-language representation learning with noisy text supervision. In *ICML*, 2021. 1
- [25] Yannis Kalantidis, Mert Bulent Sariyildiz, Noe Pion, Philippe Weinzaepfel, and Diane Larlus. Hard negative mixing for contrastive learning. In *NeurIPS*, 2020. 2
- [26] Wonjae Kim, Bokyung Son, and Ildoo Kim. Vilt: Vision-and-language transformer without convolution or region supervision. In *ICML*, 2021. 1, 2
- [27] Yangguang Li, Feng Liang, Lichen Zhao, Yufeng Cui, Wanli Ouyang, Jing Shao, Fengwei Yu, and Junjie Yan. Supervision exists everywhere: A data efficient contrastive language-image pre-training paradigm. In *ICLR*, 2022. 1, 2
- [28] Tsung-Yi Lin, Michael Maire, Serge Belongie, James Hays, Pietro Perona, Deva Ramanan, Piotr Dollár, and C Lawrence Zitnick. Microsoft coco: Common objects in context. In *ECCV*, 2014. 8
- [29] Ilya Loshchilov and Frank Hutter. Decoupled weight decay regularization. In *ICLR*, 2017. 9
- [30] Norman Mu, Alexander Kirillov, David Wagner, and Saining Xie. Slip: Self-supervision meets language-image pre-training. In *ECCV*, 2022. 1, 2, 3
- [31] Zhiliang Peng, Li Dong, Hangbo Bao, Qixiang Ye, and Furu Wei. BEiT v2: Masked image modeling with vector-quantized visual tokenizers. In *NeurIPS*, 2022. 1, 10
- [32] Alec Radford, Jong Wook Kim, Chris Hallacy, Aditya Ramesh, Gabriel Goh, Sandhini Agarwal, Girish Sastry, Amanda Askell, Pamela Mishkin, Jack Clark, et al. Learning transferable visual models from natural language supervision. In *ICML*, 2021. 1, 2, 3
- [33] Aditya Ramesh, Prafulla Dhariwal, Alex Nichol, Casey Chu, and Mark Chen. Hierarchical text-conditional image generation with clip latents. *arXiv:2204.06125*, 2022. 2
- [34] Christoph Schuhmann, Richard Vencu, Romain Beaumont, Robert Kaczmarczyk, Clayton Mullis, Aarush Katta, Theo Coombes, Jenia Jitsev, and Aran Komatsuzaki. Laion-400m: Open dataset of clip-filtered 400 million image-text pairs. In *NeurIPS Workshop*, 2021. 1, 2
- [35] Piyush Sharma, Nan Ding, Sebastian Goodman, and Radu Soricut. Conceptual captions: A cleaned, hypernymed, image alt-text dataset for automatic image captioning. In *ACL*, 2018. 1, 2, 3, 5
- [36] Zhiqiang Shen, Zechun Liu, Zhuang Liu, Marios Savvides, Trevor Darrell, and Eric Xing. Un-mix: Rethinking image mixtures for unsupervised visual representation learning. In *AAAI*, 2022. 1, 2
- [37] Ravid Shwartz-Ziv and Naftali Tishby. Opening the black box of deep neural networks via information. *arXiv:1703.00810*, 2017. 2, 4
- [38] Bart Thomee, David A Shamma, Gerald Friedland, Benjamin Elizalde, Karl Ni, Douglas Poland, Damian Borth, and Li-Jia Li. Yfcc100m: The new data in multimedia research. *Communications of the ACM*, 2016. 1
- [39] Naftali Tishby and Noga Zaslavsky. Deep learning and the information bottleneck principle. In *ITW*, 2015. 2, 4
- [40] H Touvron, M Cord, M Douze, F Massa, and A Sablayrolles. Training data-efficient image transformers & distillation through attention. In *ICML*, 2020. 2, 9
- [41] Aaron Van Den Oord, Oriol Vinyals, et al. Neural discrete representation learning. *NeurIPS*, 2017. 2
- [42] Grant Van Horn, Oisín Mac Aodha, Yang Song, Yin Cui, Chen Sun, Alex Shepard, Hartwig Adam, Pietro Perona, and Serge Belongie. The inaturalist species classification and detection dataset. In *CVPR*, 2018. 6

- [43] Ashish Vaswani, Noam Shazeer, Niki Parmar, Jakob Uszkoreit, Llion Jones, Aidan N Gomez, Łukasz Kaiser, and Illia Polosukhin. Attention is all you need. In *NeurIPS*, 2017. 2, 5
- [44] Xinlong Wang, Rufeng Zhang, Chunhua Shen, Tao Kong, and Lei Li. Dense contrastive learning for self-supervised visual pre-training. In *CVPR*, 2021. 2
- [45] Zirui Wang, Jiahui Yu, Adams Wei Yu, Zihang Dai, Yulia Tsvetkov, and Yuan Cao. SimVLM: Simple visual language model pretraining with weak supervision. In *ICLR*, 2022. 5
- [46] Chen Wei, Haoqi Fan, Saining Xie, Chao-Yuan Wu, Alan Yuille, and Christoph Feichtenhofer. Masked feature prediction for self-supervised visual pre-training. In *CVPR*, 2022. 1
- [47] Xin Wen, Bingchen Zhao, Anlin Zheng, Xiangyu Zhang, and Xiaojuan Qi. Self-supervised visual representation learning with semantic grouping. In *NeurIPS*, 2022. 2
- [48] Ronald J Williams and David Zipser. A learning algorithm for continually running fully recurrent neural networks. *Neural computation*, 1989. 5
- [49] Zhirong Wu, Yuanjun Xiong, Stella X Yu, and Dahua Lin. Unsupervised feature learning via non-parametric instance discrimination. In *CVPR*, 2018. 2
- [50] Tete Xiao, Yingcheng Liu, Bolei Zhou, Yuning Jiang, and Jian Sun. Unified perceptual parsing for scene understanding. In *ECCV*, 2018. 7
- [51] Jiahao Xie, Xiaohang Zhan, Ziwei Liu, Yew Soon Ong, and Chen Change Loy. Unsupervised object-level representation learning from scene images. In *NeurIPS*, 2021. 1
- [52] Zhenda Xie, Yutong Lin, Zheng Zhang, Yue Cao, Stephen Lin, and Han Hu. Propagate yourself: Exploring pixel-level consistency for unsupervised visual representation learning. In *CVPR*, 2021. 2
- [53] Zhenda Xie, Zheng Zhang, Yue Cao, Yutong Lin, Jianmin Bao, Zhuliang Yao, Qi Dai, and Han Hu. Simmim: A simple framework for masked image modeling. In *CVPR*, 2022. 2
- [54] Lewei Yao, Runhui Huang, Lu Hou, Guansong Lu, Minzhe Niu, Hang Xu, Xiaodan Liang, Zhenguo Li, Xin Jiang, and Chunjing Xu. FILIP: Fine-grained interactive language-image pre-training. In *ICLR*, 2022. 1, 2
- [55] Jiahui Yu, Zirui Wang, Vijay Vasudevan, Legg Yeung, Mojtaba Seyedhosseini, and Yonghui Wu. CoCa: Contrastive captioners are image-text foundation models. *arXiv:2205.01917*, 2022. 2, 3
- [56] Bingchen Zhao and Xin Wen. Distilling visual priors from self-supervised learning. In *European Conference on Computer Vision*, pages 422–429. Springer, 2020. 2
- [57] Bolei Zhou, Agata Lapedriza, Aditya Khosla, Aude Oliva, and Antonio Torralba. Places: A 10 million image database for scene recognition. *IEEE TPAMI*, 2017. 6
- [58] Bolei Zhou, Hang Zhao, Xavier Puig, Sanja Fidler, Adela Barriuso, and Antonio Torralba. Scene parsing through ade20k dataset. In *CVPR*, 2017. 7
- [59] Rui Zhu, Bingchen Zhao, Jingen Liu, Zhenglong Sun, and Chang Wen Chen. Improving contrastive learning by visualizing feature transformation. In *ICCV*, 2021. 2